
Taylor & Francis
Taylor & Francis Group

Plastics, Rubber and Composites
Macromolecular Engineering

ISSN: 1465-8011 (Print) 1743-2898 (Online) Journal homepage: http://www.tandfonline.com/loi/yprc20

# Production of cellulose nanofibers from Alfa grass and application as reinforcement for polyvinyl alcohol

Salma Ben Cheikh, Ridha Ben Cheikh, Eunice Cunha, Paulo E. Lopes & Maria C. Paiva

**To cite this article:** Salma Ben Cheikh, Ridha Ben Cheikh, Eunice Cunha, Paulo E. Lopes & Maria C. Paiva (2018) Production of cellulose nanofibers from Alfa grass and application as reinforcement for polyvinyl alcohol, Plastics, Rubber and Composites, 47:7, 297-305, DOI: 10.1080/14658011.2018.1479822

**To link to this article:** https://doi.org/10.1080/14658011.2018.1479822

PLASTICS, RUBBER AND COMPOSITES
2018, VOL. 47, NO. 7, 297–305
https://doi.org/10.1080/14658011.2018.1479822

The Institute of Materials, Minerals and Mining

Taylor & Francis
Taylor & Francis Group



# Production of cellulose nanofibers from Alfa grass and application as reinforcement for polyvinyl alcohol

Salma Ben Cheikh[a], Ridha Ben Cheikh[a], Eunice Cunha[b], Paulo E. Lopes[b] and Maria C. Paiva[b]

[a]Laboratoire de Matériaux, Optimisation et Energie pour la Durabilité, Ecole Nationale d'Ingénieurs de Tunis, Université Tunis El Manar, Tunis, Tunisia; [b]Department of Polymer Engineering, Institute for Polymers and Composites, University of Minho, Guimarães, Portugal

**ABSTRACT**

The work reported demonstrates an simple method of extracting cellulose nanofibers (CNF) from cellulose microfibers (CMF) obtained from the plant *Stipatenacissima*. Here, a method for the production of CNF from CMF extracted from Alfa grass by exfoliation in polyvinyl alcohol (PVA) solution, is demonstrated. The CMF were produced in powder form and exfoliated in PVA aqueous solution to produce composites with 2, 4, 5 and 10 wt-% of CNF. Scanning Electron Microscopy demonstrated exfoliation of CMF, dispersion of the CNF and wetting by the polymer. The composites were characterised by thermogravimetry, differential scanning calorimetry, X-ray diffraction and tensile testing. The addition of CNF to PVA reduced the crystallinity degree of PVA. The large increase of the Young's modulus from 38 to 113% (relative to pure PVA) for composites with 2 to 10 wt-% of CNF incorporation is consistent with the extensive exfoliation of CMF into CNF and its excellent interface with PVA.

**ARTICLE HISTORY**
Received 10 December 2017
Revised 1 May 2018
Accepted 11 May 2018

**KEYWORDS**
Alfa; cellulose; microfibers; nanofibers; nanocomposite; polyvinyl alcohol

## Introduction

In these few last decades, there is a growing interest in nanomaterials and fabricating products based on natural resources that can reduce the dependence on fossil fuel and decrease the pollution impact [1,2]. In parallel, researchers have focused their works on designing and producing bio-nanocomposite materials which are a new generation of nanostructured hybrid materials containing natural fillers with at least one dimension smaller than 100 nm [3–6].

The use of cellulose nanofibers (CNF) as a reinforcing agent in polymer nanocomposites has drawn an increasing attention because of their biodegradability, renewability, low density, nontoxicity, high stiffness, low cost and their high surface area to volume ratio [7–9].

Currently, CNF can be produced from various resources, such as wood [10], cotton [11], ramie [12], bacterial cellulose [13] and microcrystalline cellulose [14,15] using different methods such as the acid hydrolysis process [16–18] which is the most common preparation method employed to extract CNF, high pressure homogenisation [19–21] and cryocrushing [22,23].

Recently, the application of ultrasounds to cellulose fibre suspensions has been used in order to extract CNF [24–26]. All these methods lead to different types of CNF, depending on the cellulose raw materials, its pre-treatment, and on the disintegration process [27]. The use of Alfa fibres to produce nanocomposites using thermoplastic materials has been recently published [28–30].

With the aim of developing and improving the properties of a new nanostructured green hybrid material and valorising natural resources in the less industrialised countries, we investigated the preparation of nanocomposites reinforced with cellulosic nanofibers extracted from Tunisian Alfa plants.

Polyvinyl alcohol (PVA)-based nanocomposites have been considered as an attractive choice in tissue scaffolding, filtration materials, membranes, optics, protective clothing, enzyme immobilisation, drug release hydrogel, membrane material for chemical separation, barrier membrane for food packaging, pharmaceutical component, manufacturing material for artificial human organs and biomaterials [31–34]. It is a water-soluble polymer and is considered as a good candidate for the fabrication of composites reinforced with CNF.

The extraction of CNF from the bleached and delignified Alfa fibres was described by Ben Mabrouk et al. [35]. In this work, a new procedure has been followed to form CNF from the dried cellulose microfibers (CMF) extracted from Alfa fibres and incorporated in PVA. The nanocomposite and the CNF were obtained via the ultrasonication of their aqueous suspensions and were fully characterised by scanning electron microscopy (SEM), differential scanning calorimetry(DSC), thermogravimetric analysis (TGA), X-ray diffraction (XRD) and tensile tests. The results

**CONTACT** Maria C. Paiva mcpaiva@dep.uminho.pt Department of Polymer Engineering, Institute for Polymers and Composites, University of Minho, 4800-058 Guimarães, Portugal

obtained demonstrate a simple and ecological method to exfoliate CMF powder, extracted from Alfa grass, into CNF in PVA solution. Total exfoliation of CMF is achieved, forming stable CNF suspensions in PVA even at high CNF loadings. Moreover, the nanocomposite films formed show transparency and an excellent CNF/PVA interface, maintaining biocompatibility and largely increasing mechanical performance, opening vast possibilities in biomedical applications.

## Experimental

### Materials

Alfa stems collected in the region of Kasserine (Tunisia) were used as raw material for extraction of CNF. PVA (PVA05-99 from SUNDY) was used as a matrix in all composites.

### Isolation of CMF from Alfa

The extraction of CMF from Alfa plant was carried out following a protocol that was described by Ben Brahim and Ben Cheikh [28] and Gherissi et al. [30].

This process consists of cooking the plant stem in a 3N NaOH solution for 2 h under atmospheric pressure and a temperature of 100°C then bleaching in a 50% (v/v) NaClO solution for 1 h. The fibres obtained were washed abundantly with water until pH 7 and dried at 80°C for 48 h.

The obtained Alfa paste was hydrolysed in a 50% (v/v) sulphuric acid solution for 30 min at 70°C, the excess of sulphuric acid was removed from the sediment by repeated cycles of centrifugation for 15 min at 10000 rev $min^{-1}$. After acid hydrolysis and centrifugation, the cellulosic microfibers were dried for 24 h at 40°C, crushed to a fine powder, and investigated for morphology by SEM and XRD.

### Preparation of CNF and PVA/cellulose nanofiber composites

A new procedure for the preparation of CNF and PVA nanocomposites was implemented that consisted on mixing the CMF powder obtained as described in the previous section directly with the polymer solution, and treating the obtained suspension with ultrasounds for 1 h. The CMF exfoliation was induced and the CNF were dispersed in the polymer solution as soon as they were formed.

The preparation of the polymer solution was carried out by dissolving 2 g of PVA in 100 mL distilled water at 90°C and magnetic stirring for 1 h. Different weights of the CMF powder were added to the PVA solution, magnetically stirred for 15 min and sonicated for 1 h using a Hielscher Ultrasonic processor UP100H equipped with a sonotrode MS2. The homogeneous suspensions were cast on glass plates and dried at room temperature for 24 h. The nanocomposite films were produced with nominal CNF weight of 2, 4, 5 and 10%, and the composites were labelled PVA/CNF2, PVA/CNF4, PVA/CNF5 and PVA/CNF10, respectively. An alternative procedure for the CNF and composite production was carried by preparing an aqueous suspension of CMF previously obtained, applying ultrasounds for 2 h and then adding to the polymer solution to produce a nanocomposite with nominal 4 wt-%CNF, for comparison with the PVA/CNF composites prepared by direct mixing in the polymer solution.The XRD analysis performed (see sections 'X-ray diffraction' and 'X-ray diffraction analysis') allowed the exact determination of the CNF content achieved in each composite prepared. However, the nomenclature for composite designation was kept as indicated above.

### Characterisation

#### Scanning electron microscopy

SEM observation was performed oncryo-fractured samples. The composite films were immersed in liquid nitrogen and fractured for the observation of the cross-section. The cryo-fractured surfaces were coated with a thin layer of gold and observed by SEM on a NanoSEM FEI Nova 200 microscope.

#### Thermogravimetric analysis

The thermal stability of both pure PVA and nanocomposite films was investigated by thermogravimetric analysis on a Q500 equipment from TA Instruments. The samples were heated from 40 to 800°C, at a heating rate of 10°C $min^{-1}$. The tests were performed under a constant nitrogen flow of 60 mL $min^{-1}$.

#### Differential scanning calorimetry

DSC analyses were performed under nitrogen flow in the temperature range of 0–250°C on a Perkin Elmer Diamond Pyris equipment. Samples were heated to 250°C and held at that temperature for 2 min, in order to remove any previous thermal history, then cooled from the melt to 0°C, and heated again to 250°C, the scanning rates for heating and cooling during DSC measurements were set at 10°C $min^{-1}$.

According to Young Yu et al. [36], the degree of crystallinity ($\chi_C$) of the polymer before and after the addition of CNF was calculated as represented in Equation (1).

$$\chi_c(\%) = \frac{\Delta H_m}{(1-\Phi)\times \Delta H_{100}} \times 100 \qquad (1)$$

where $\Phi$ is the weight fraction of the CNF in the

composites, $\Delta H_m$ is the melting enthalpy of the analysed samples (J $g^{-1}$), and according to Jelinska et al. [37], $\Delta H_{100}$ was considered as138 J $g^{-1}$ for the melting enthalpy of 100% crystalline PVA.

### X-Ray diffraction

PVA, CNF and their composites were analysed by XRD on a Bruker D8 Discover using a Cu Kα radiation with a Ni filter. The X-ray data were fitted with Gaussian functions for the PVA and cellulose reinforcement individually. The composites data were fitted using the PVA and cellulose individually fitted profiles, and the resulting data were used to estimate the CNF content.

### Tensile tests

Tensile properties of nanocomposite films were measured according to ASTM D882. Tensile tests are carried out at ambient conditions on an Instron 4505 universal testing machine. The test specimens were rectangular, with 5 mm width and an approximate thickness of 70 µm, and were tested at an initial gauge length of 30 mm. The exact specimen thickness was measured immediately before the test was performed. A fixed crosshead speed of 3 mm $min^{-1}$ was used.

## Results and discussion

### Scanning electron microscopy

Figure 1. A and B show SEM micrographs of Alfa CMF after chemical treatment. Most of the Alfa stem's components were dissolved, leaving the smooth, individualised and uniform cellulose fibres, showing that the chemical treatment with sodium hydroxide and sulphuric acid did not destroy the cellulose fibres [27]. The electron micrograph revealed that before ultrasonication the cellulose filaments presented a diameter in the scale of tens of micrometres (Figure 1(a,b)). From Figure 1(b), the cross-section of the singular microfiber shows that this fibre is itself

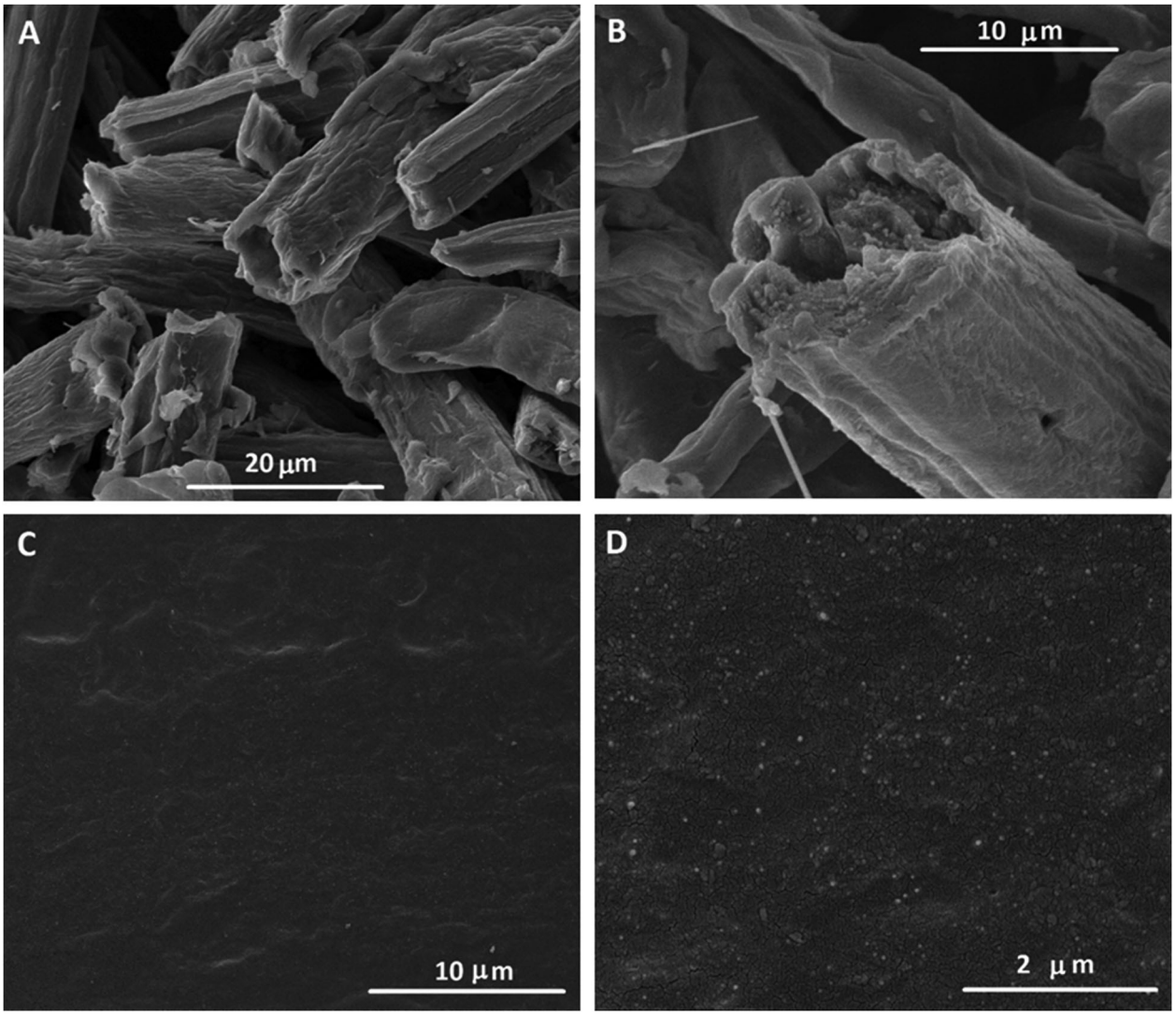


**Figure 1.** SEM micrographs of: (A) purified CMF; (B) cross-section of a CMF after acid hydrolysis; (C,D) cross-section of PVA reinforced with 10 wt-% CNF.

tubular and the wall is composed of fibrils with very small dimension. This observation is in accordance with the literature indicating that the fibrils are linked to each other by intermolecular hydrogen bonds [5].

Figure 1(c,d) shows that the nanocomposites reinforced with10 wt-% of CNF reveal a good distribution of the nanofiller in the PVA matrix which was homogeneously dispersed. The fractured surface was smooth and did not show the presence of large micron-scale fibres (Figure 1(c)), containing mostly CNF that were well distributed and embedded in the matrix, demonstrating a good CNF/PVA interface (Figure 1(d)). Similar results were observed for the composites with lower CNF compositions.

Considering the size of the filament tips observed along the cross-section of the composite cryo-fracture, it may be concluded that the CMF went through an exfoliation process, yielding CNF with diameters in the order of 40 nm. Even for the larger CNF concentration 10 wt-% (Figure 1(d)), there was no observation of CNF agglomeration at the micron scale.

## Thermogravimetric analysis

Figure 2(a,b) presents the TGA and corresponding derivative (DTG) curves of CNF showing two stages of weight loss within the temperature range 40–550°C. The first thermal degradation stage is observed within the temperature range 100–250°C and the second within 250–550°C, due to the degradation processes of cellulose, such as dehydration, decarboxylation, depolymerisation and decomposition of glycosyl units, [27] as shown on the DTG curve (Figure 2(b)), the maximum degradation rate occurs at approximately 190°C for the first degradation step.

Figure 2 presents the TGA and corresponding DTG curves for CNF (cellulose) (A and B), and the TGA and corresponding DTG curves for PVA and PVA/CNF nanocomposite films (C and D). The relevant degradation temperatures obtained from the TGA analysis are presented in Table 1. It was observed that PVA and its nanocomposites present three major weight loss steps within the temperature range 40–550°C. First, a drying stage occurs within the temperature range 40–115°C due to the evaporation of adsorbed moisture that may account for 5–6% of the weight loss.Thermal degradation of PVA occurred in two stages, within the temperature ranges of 150–380°C and 380–550°C. The first stage involves a weight loss of approximately 74% (Table 1), and may correspond to degradation of PVA via elimination of water from PVA molecules and formation of a polyene intermediate; during the second thermal degradation stage the polyene may be subjected to chain scission and molecular degradation corresponding to approximately

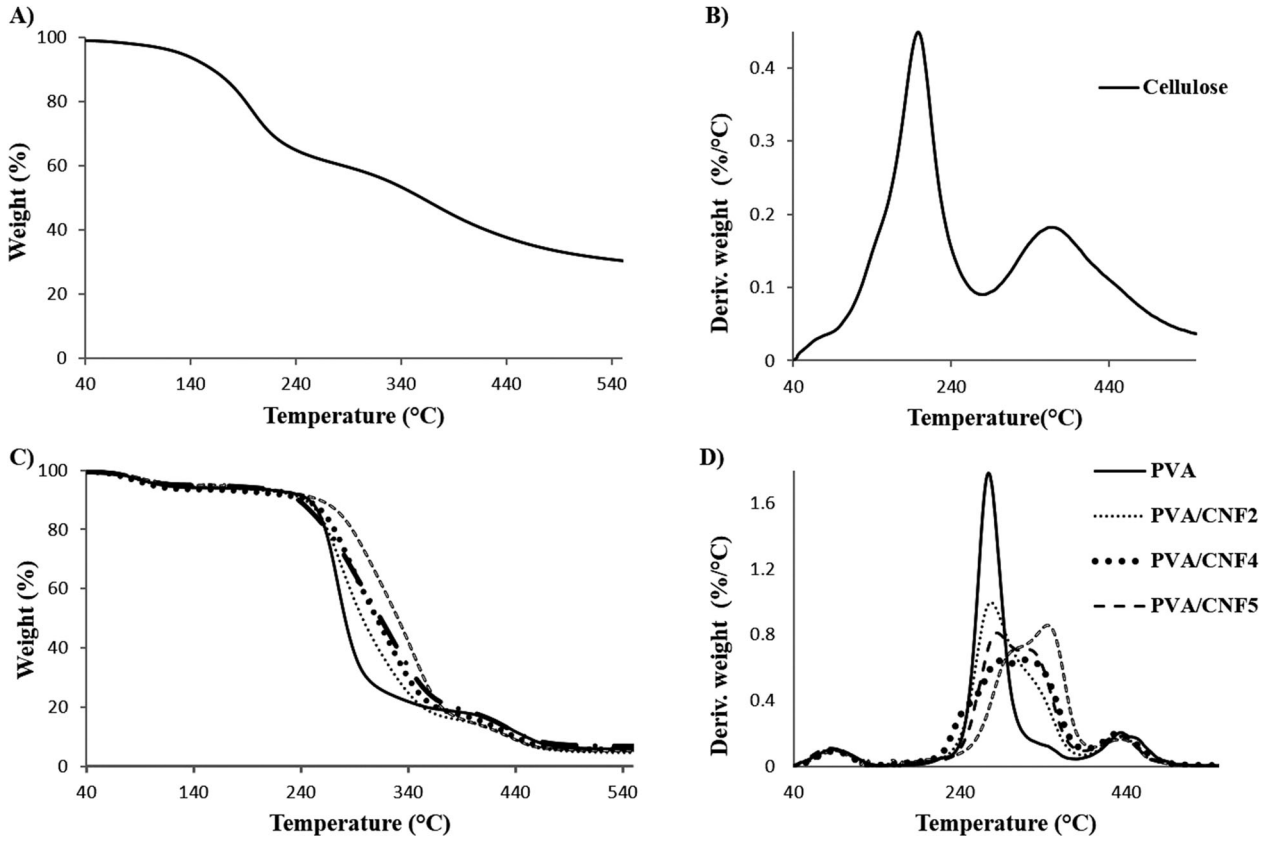


**Figure 2.** TGA and corresponding DTG curves for CNF (cellulose) (A,B);TGA and corresponding DTG curves for PVA and PVA/CNF nanocomposite films (C,D).

**Table 1.** Thermal parameters obtained from the TGA/DTG curves of neat PVA and its CNF nanocomposite films.

| | Onset temperature (°C) | DTG peak temperature (°C) | Weight loss at 800°C (%) |
|---|---|---|---|
| PVA | 253.5 | 272.5 | 73.5 |
| PVA/CNF2 | 245.5 | 273.0 | 73.9 |
| PVA/CNF4 | 235.0 | 319.5 | 73.3 |
| PVA/CNF5 | 247.5 | 284.7 | 74.4 |
| PVA/CNF10 | 271.5 | 339.0 | 77.2 |

**Table 2.** Thermal characteristics of PVA and its nanocomposites obtained from DSC.

| | $T_g$ (°C) | $T_m$ (°C) | $\Delta H_m$ (J g$^{-1}$) | $\chi_c$ (%) |
|---|---|---|---|---|
| PVA | 73.5 | 225.9 | 66.1 | 47.9 |
| PVA/CNF2 | 73.2 | 224.1 | 55.1 | 40.7 |
| PVA/CNF4 | 78.6 | 224.0 | 45.9 | 34.7 |
| PVA/CNF5 | 78.0 | 223.8 | 49.5 | 37.7 |
| PVA/CNF10 | 77.1 | 219.4 | 42.6 | 34.3 |

15% of weight loss, leaving a solid char residue, in agreement with the results reported by Yuwawech et al. [38]

The nanocomposites present two degradation steps within the temperature range of 150–550°C, showing the first PVA/CNF degradation step shifted to a considerably higher temperature compared to neat PVA. Thus, the addition of increasing amounts of CNF to PVA induced a progressive increase in degradation temperature compared to neat PVA, and a decrease in the degradation rate. This observation is in line with the results reported by Li et al. [18].

Figure 2(d) shows that the temperature of maximum decomposition rate increased from 272.5°C for neat PVA to 339°C (Table 1) for PVA/CNF10, while the decomposition rate decreased after the addition of CNF. These effects may be ascribed to the restriction of mobility of PVA chains caused by the homogeneous distribution of CNF in the polymer previously observed in SEM images (Figure 1), as well as to a barrier effect of the nanofillers to the diffusion of the decomposition gases. Similar effects were observed in other studies [39,40].

## Differential scanning calorimetry

Crystallinity is an important parameter, which can greatly affect the physical properties of polymers. Therefore, the crystallization behaviour of neat PVA and the nanocomposites with various CNF contents was investigated by DSC.

The DSC thermograms of neat PVA films and nanocomposites are shown in (Figure 3). The crystallinity of PVA was calculated from the DSC curves and the results are presented in Table 2. Table 2 summarises the major thermal parameters obtained from the

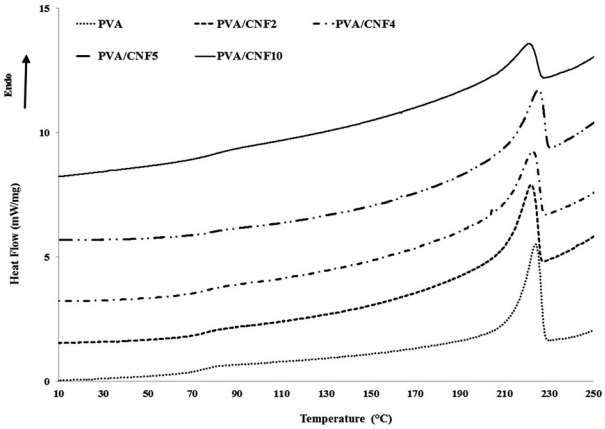


**Figure 3.** DSC curves obtained for neat PVA and PVA/CNF nanocomposite films.

DSC thermograms, namely the melting enthalpy ($\Delta H_m$), the degree of crystallinity ($\chi_c$) and the glass transition temperature ($T_g$). The melting enthalpy reduced from 66.1 to 42.6 J g$^{-1}$, corresponding to a decrease of the degree of crystallinity from 47.9 to 34.3%, for neat PVA and for PVA reinforced with10% CNF, respectively. As discussed above for the TGA results, this may be a consequence of the limited mobility of PVA chains in the presence of CNF, disturbing the ability for molecular organisation, resulting in a decrease of the overall polymer crystallinity in the nanocomposites. In this work, the melting temperature decreased from 225.9°C for neat PVA to 219.5°C for PVA reinforced with 10% CNF, illustrating the lower lamella thickness of PVA crystals caused by the addition of CNF to the polymer, and this is consistent with the studies elaborated by Yu et al. [36] and Ten et al. [40].

The glass transition temperature increased from 73.5°C for neat PVA to 77.1°C for PVA reinforced with 10 wt-% CNF, and this trend is also in agreement with restrained mobility of PVA chains after the addition of CNF. Similar results were reported in other studies [41,42].

## XRD analysis

XRD analysis of the neat PVA polymer, the neat CMF, and neat CNF and the PVA/CNF nanocomposites, produced the intensity profiles presented in Figure 4(a,b). CNF were obtained after treating an aqueous suspension of CMF with ultrasounds and drying the exfoliated product. Both neat CMF and neat CNF X-ray profiles present three peaks, as depicted in Figure 4(a), the two peaks at 15.4° and 16.6° in $2\theta$ appear for both materials, however with different intensity ratios indicate that the ultrasound removed part of the amorphous portion of CMF [43]. The higher intensity peak at 22.8° in $2\theta$ has similar characteristics for CNF and CMF

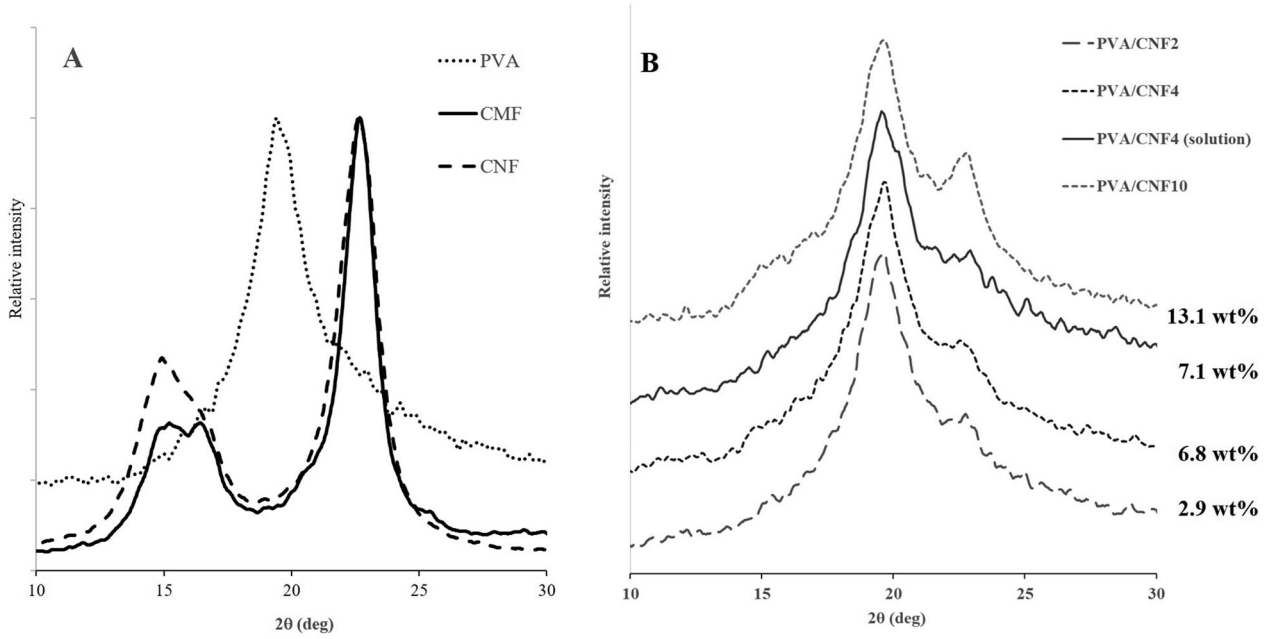


**Figure 4.** Wide-angle XRD patterns of (A) PVA, CMF and CNF; (B) PVA composites with different CNF composition.

showing the crystallinity of both cellulosic nanofibers and cellulosic microfibers. These diffraction three peaks are typical of cellulose I according to Hasan et al. [44,45].

The PVA/CNF composites X-ray profiles obtained were fitted with the individual profiles of PVA and CNF to estimate the weight % reinforcement content. A composite with 4 wt-% of CNF was prepared by mixing a CNF suspension, previously obtained by exfoliation of CMF in water using ultrasounds, with the PVA solution. This procedure for composite preparation was compared to the procedure described in the experimental section (direct addition of the CMF powder to the PVA solution and exfoliation by ultrasounds). Both procedures yielded similar CNF contents and formed homogeneous composites, as those depicted in Figure 1.

X-ray profiles of the PVA–CNF composites, (Figure 4(b)), present the characteristic peak of the polymer and a small peak at 22.8° in $2\theta$ from the CNF [43–45] that increases with increasing CNF content. The content values obtained from the fitting of the composites X-ray profiles are presented in (Figure 4(b)) next to the respective line (2.9, 6.8, 7.1 and 13.1)%, and are systematically higher than the target content of the nanocomposite (2, 4, 4 and 10)%, these variations are attributed to the experimental procedures. The application of ultrasounds on the CMF suspension before addition to the polymer solution does not affect the dispersion of CNF in the polymer and thus is not required for the nanocomposite preparation, showing that the major factor for the successful exfoliation of CMF into CNF is related to the strong interactions between CNF and PVA in aqueous solution.

## *Tensile testing*

The mechanical properties of PVA and nanocomposite films were characterised by tensile testing. Figure 5 illustrates the stress–strain curves of PVA and its nanocomposites.

A significant increase of the Young's modulus was observed for the composites relative to pure PVA after the addition of CNF, as depicted in Figure 6. The addition of only 2 wt-% of CNF induced an increase of 38% in the Young's modulus, while the addition of 5 and 10 wt-% of CNF led to increases of 75 and 113%, respectively. The large increase observed in the composite modulus is due to the excellent mechanical properties of the CNF. The CNF constitute the reinforcing phase of the CMF, and the mechanical properties of the latter were evaluated experimentally, demonstrating a tensile modulus near 20 GPa and tensile strength higher than 240 MPa [46]. Additionally, the chemical compatibility of CNF and PVA due to the presence of hydroxyl groups in the composition

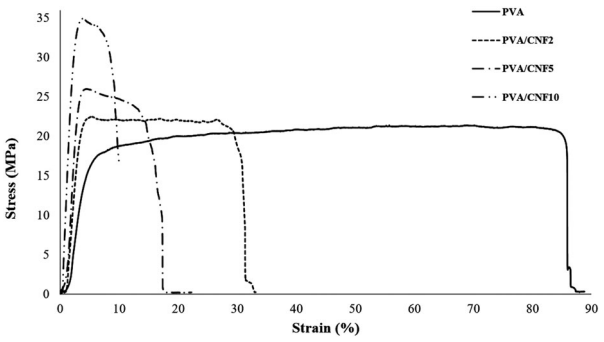


**Figure 5.** Stress–strain curves of neat PVA and its nanocomposite films.

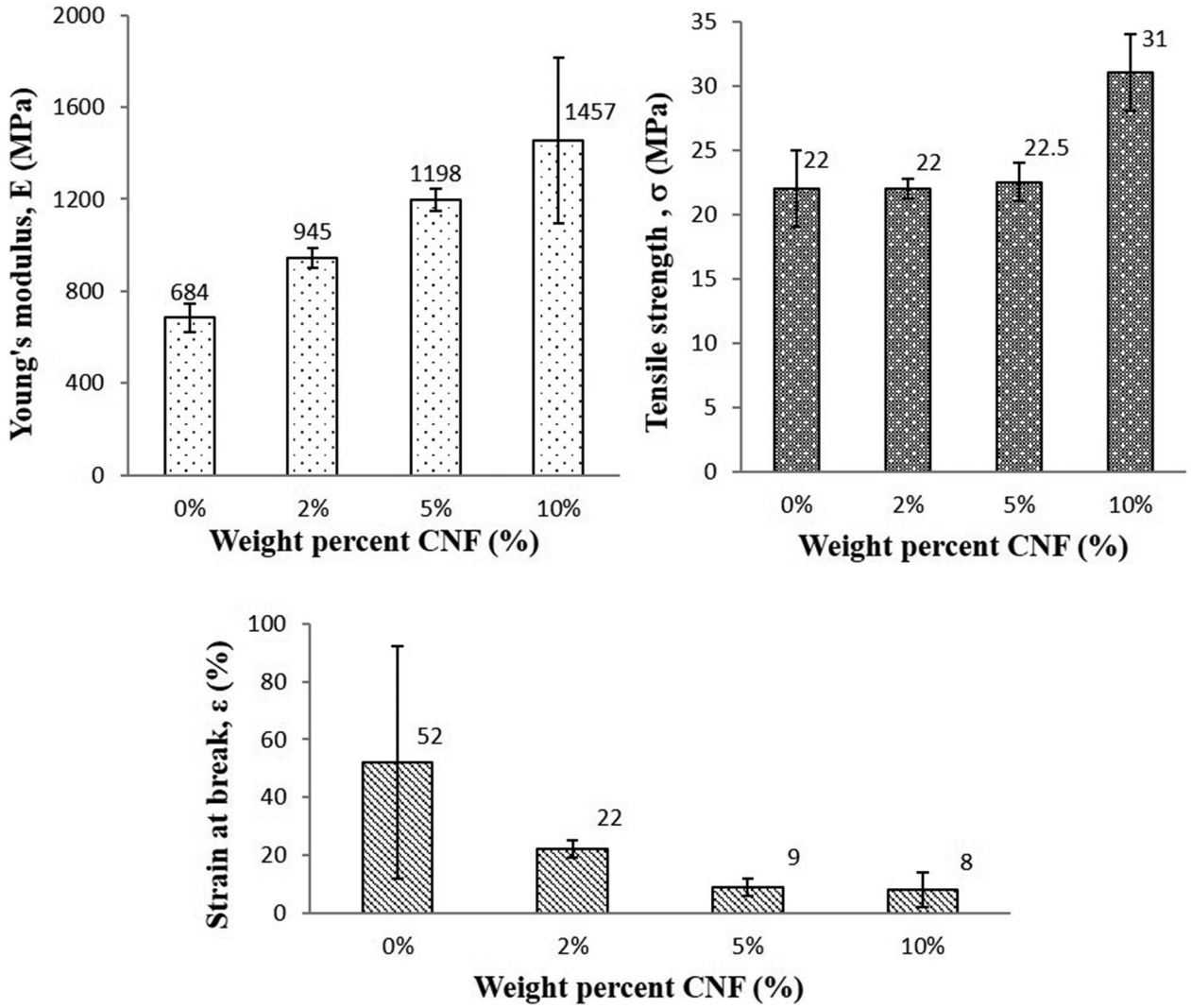


**Figure 6.** Young's modulus ($E$), tensile strength ($\sigma$) and strain at break ($\varepsilon$) of neat PVA and PVA/CNF nanocomposite films.

of both materials and the possibility of strong hydrogen bonding between the PVA hydroxyl groups and cellulose results in good adhesion, as demonstrated by SEM observations (Figure 1). Considering all these aspects and the good dispersion of CNF in PVA even at high CNF concentration, the large improvement in composite mechanical properties as well as thermal properties previously studied by TGA (Figure 2) was expected [38–47].

The tensile strength of the composites showed little improvement at low CNF content, however, at higher content, the improvement reached 41% relative to pure PVA.

Finally, the composites strain at break was observed to decrease considerably with the increase in CNF content. A large decrease in ductility is expected for composites formed by a ductile matrix and a highly stiff, brittle reinforcing phase. The CNF properties are transferred to the composite, and this transfer is more effective when there is a high level of adhesion between the polymer and nanofilament (Figure 1). Since the CNF are stiff, brittle and strongly interacting with the PVA molecules at the interface, these molecules lose mobility as was previously interpreted and the composite elongation at break as well as other thermal parameters previously studied decreases extensively as the CNF content is increased [39].

## Conclusions

CMF were prepared from Alfa fibres by application of a soda process followed by acid hydrolysis. The CMF powder obtained was then mixed with PVA aqueous solution at CMF contents ranging between 2 and 10%, ultrasounds were applied to induce the separation of CMF into the individual CNF. Transparent, homogeneous nanocomposite films were produced by solvent casting. SEM observation demonstrated the absence of CMF that were exfoliated into CNF, which were well distributed and dispersed in the PVA matrix. DSC analysis indicated a decrease in PVA crystallinity, while the glass transition temperature increased with CNF content. TGA results showed that the addition of CNF increased the thermal stability of PVA composites. XRD results showed differences in the intensity profiles obtained for CMF and CNF, and allowed

determining the exact CNF content of the nanocomposites. The addition of CNF to PVA largely improved the mechanical properties of the nanocomposites, increasing the Young's modulus and the tensile strength by 113 and 41%, respectively, for composites with 10 wt-% CNF.

The main conclusion of this work is that CMF produced from Alfa grass form CNF simply by mixing in PVA solution and applying ultrasounds for a short period. The CNF produced present an excellent mechanical reinforcement effect while maintaining film transparency. These nanocomposite films with enhanced properties maintain the biocompatibility characteristics of PVA, opening vast possibilities in biomedical applications.

## Disclosure statement

No potential conflict of interest was reported by the authors.

## Funding

The authors acknowledge the Portuguese Foundation for Science and Technology (FCT) for project PEst-C/CTM/LA0025/2013 (Strategic Project - LA 25 - 2013–2014). Salma Ben Cheikh acknowledges the Ministry of Higher Education and Scientific Research (Tunisia) for a grant to travel to IPC/i3N in Portugal.

## References

[1] Pandly JK, Kumar AP, Misra M, et al. Recent advances in biodegradable nanocomposites. J Nanosci Nanotechnol. 2005;32:497–526.
[2] Espert A, Vilaplana F, Karlsson S. Comparison of water absorption in natural cellulosic fibres from wood and one-year crops in polypropylene composites and its influence on their mechanical properties. Compos Part A Appl Sci Manuf. 2004;35:1267–1276.
[3] Dufresne A. Comparing the mechanical properties of high performances polymer nanocomposites from biological sources. J Nanosci Nanotechnol. 2006;6:322–330.
[4] Camargo PHC, Satyanarayana KG, Wypych F. Nanocomposites: synthesis, structure, properties and new application opportunities. J Mater Res. 2009;12:1–39.
[5] Siqueira G, Bras J, Dufresne A. Cellulosic bionanocomposite: a review of preparation. properties and applications. Polymer. 2010;2:728–765.
[6] Adeosun SO, Lawal GI, Balogun SA, et al. Review of green polymer nanocomposites. J Miner Mater Char Eng. 2012;11:385–416.
[7] Kalia S, Dufresne A, Cherian BM, et al. Cellulose-based bio- and nanocomposites: a review. Int J Polym Sci. 2011;2011:1–35.
[8] Abilash N, Sivapragash M. Environmental benefits of eco-friendly natural fiber reinforced polymeric composite materials. Int J App Innov Eng Manag. 2013;2:2319–4847.
[9] Persesin MS, Habibi Y, Zoppe JO, et al. Nanofiber composites of polyvinyl alcohol and cellulose nanocrystals: manufacture and characterization. Biomacromolecules. 2010;11:674–681.
[10] Revol JF, Bradford H, Giasson J, et al. Helicoidal self-ordering of cellulose microfibrils in aqueous suspension. Int J Biol Macromol. 1992;14:170–172.
[11] Dong XM, Revol JF, Gray DG. Effect of microcrystallite preparation conditions on the formation of colloid crystals of cellulose. Cellulose. 1998;5:19–32.
[12] Moran JI, Alvarez VA, Cyras VP, et al. Extraction of cellulose and preparation of nanocellulose from sisal fibers. Cellulose. 2008;15:149–159.
[13] Araki J, Kuga S. Effect of trace electrolyte on liquid crystal type of cellulose, microcrystals. Langmuir. 2001;17:4493–4496.
[14] Roman M, Winter WT. Effect of sulfate groups from sulfuric acid hydrolysis on the thermal degradation behavior of bacterial cellulose. Biomacromolecules. 2004;5:1671–1677.
[15] Bondeson D, Mathew A, Oksman K. Optimization of the isolation of nanocrystals from microcrystalline cellulose by acid hydrolysis. Cellulose. 2006;13:171–180.
[16] Marchessault RH, Morehead FF, Walter NM. Liquid crystal systems from fibrillar polysaccharides. Nature. 1959;184:632–633.
[17] Xiang Q, Lee YY, Pettersson PO, et al. Heterogeneous aspects of acid hydrolysis of α-cellulose. Appl Biochem Biotechnol. 2003;107:105–108.
[18] Li W, Yue J, Liu S. Preparation of nanocrystalline cellulose via ultrasound and its reinforcement capability for poly(vinyl alcohol) composites. Ultrason Sonochem. 2012;19:479–485.
[19] Bruce DM, Hobson RN, Farrent JW, et al. High performance composites from low-cost plant primary cell walls. Compos Part A Appl Sci Manuf. 2005;36:1486–1493.
[20] Stenstad P, Andresen M, Tanem BS, et al. Chemical surface modification of microfibrillated cellulose. Cellulose. 2008;15:35–45.
[21] Leitner J, Hinterstoisser B, Wastyn M, et al. Sugar beet cellulose nanofibril-reinforced composites. Cellulose. 2007;14:419–425.
[22] Alemdar A, Sain M. Isolation and characterization of nanofibers from agricultural residues – wheat straw and soy hulls. J Bioresource Technol. 2008;99:1664–1671.
[23] Wang B, Sain M. Dispersion of soybean stock-based nanofiber in a plastic matrix. Polym Int. 2007;56:538–546.
[24] Chen WS, Yu HP, Liu YX, et al. Individualization of cellulose nanofibers from wood using high-intensity ultrasonication combined with chemical pretreatments. Carbohyd Polym. 2011;83:1804–1811.
[25] Cheng QZ, Wang SQ, Han QY. Novel process for isolating fibrils fromcellulose fibers by high-intensity ultrasonication. II. Fibril characterization. J Appl Polym Sci. 2010;115:2756–2762.
[26] Cheng QZ, Wang SQ, Rials TG. Poly(vinyl alcohol) nanocomposites reinforced with cellulose fibrils isolated by high intensity ultrasonication. Compos Part A- Appl S. 2009;40:218–224.
[27] Trache D, Donnot A, khimeche K, et al. Physico-chemical properties and thermal stability of microcrystalline cellulose isolated from Alfa fibers. Carbohyd Polym. 2014;104:223–230.
[28] Ben Brahim S, Ben Cheikh R. Influence of fibre orientation and volume fraction on the tensile properties of

unidirectional Alfa-polyester composite. Compos Sci Technol. 2007;67:140–147.
[29] Ammar I, Campos AR, Cunha AM, et al. Injection molded composites of short Alfa fibers and biodegradable blends. Polym Compos. 2006;27:341–348.
[30] Gherissi A, Ben Cheikh R, Dévaux E, et al. Cellulose whiskers micro-fibers effect on the mechanical properties of PP and PLA composite fibers obtained by spinning process. Appl Mech Mater. 2012;146:12–26.
[31] Pajak J, Ziemski M, Nowak B. Poly(vinylalcohol)-biodegradable vinyl material. Chemik. 2010;64:523–530.
[32] Lange J, Wyser Y. Recent innovations in barrier technologies for plastic packaging – a review. Packag Technol Sci. 2003;16:149–158.
[33] Schmedlen R, Masters K, West J. Photocrosslinkable polyvinyl alcohol hydrogels that can be modified with cell adhesion peptides for the use in tissue engineering. Biomaterials. 2002;23:4325–4332.
[34] Wan W, Campbell G, Zhang Z, et al. Optimizing the tensile properties of poly(vinyl alcohol) hydrogel for the construction of a bioprosthetic heart valve stent. J Biomed Mater Res. 2002;63:854–861.
[35] Ben Mabrouk A, Kaddami H, Boufi S, et al. Cellulosic nanoparticles from alfa fibers(*Stipa tenacissima*): extraction procedures and reinforcement potential in polymer nanocomposites. Cellulose. 2012;19:843–853.
[36] Yu H, Qin Z, Zhou Z. Cellulose nanocrystals as green fillers to improve crystallization and hydrophilic property of poly(3-hydroxybutyrate-co-3-hydroxyvalerate). Prog Nat Sci Mater. 2011;21:478–484.
[37] Jelinska N, Kalnins M, Tupureina V, et al. Poly(vinylalcohol)/Poly(vinylacetate) blends films. Mater Sci Appl Chem. 2010;21:55–61.
[38] Yuwawech K, Wootthikanokkhan J, Tanpichai S. Effects of two different cellulose nanofiber types on properties of poly(vinyl alcohol) composite films. J Nanomater. 2015;2015:1–10.
[39] Kakroodi AR, Cheng S, Sain M, et al. Mechanical, thermal, and morphological properties of nanocomposites based on polyvinyl alcohol and cellulose nanofiber from aloe vera rind. J Nanomater. 2014;2014:1–7.
[40] Ten E, Turtle J, Bahr D, et al. Thermal and mechanical properties of poly (3-hydroxybutyrate-co-3-hydroxyvalerate)/cellulose nanowhiskers composites. Polymer (Guildf). 2010;51:2652–2660.
[41] Cendoya I, Lopez D, Alegria A, et al. Dynamic mechanical and dielectrical properties of poly(vinyl alcohol) and poly(vinyl alcohol)-based nanocomposites. J Polym Sci Pol Phys. 2001;39:1968–1975.
[42] Bandi S, Schiraldi DA. Glass transition behavior of clay aerogel/poly (vinyl alcohol) composites. Macromolecules. 2006;39:6537–6545.
[43] Pelissari FM, Sobral PJDA, Menegalli FC. Isolation and characterization of cellulose nanofibers from banana peels. Cellulose. 2014;21:417–432.
[44] Hasan A, waibhaw G, Saxena V, et al. Nano-biocomposite scaffolds of chitosan, carboxymethyl cellulose and silver nanoparticle modified cellulose nanowhiskers for bone tissue engineering applications. Int J Biol Macromol. 2018;111:923–934.
[45] Hasan A, Waibhaw G, Tiwari S, et al. Fabrication and characterization of chitosan, polyvinylpyrrolidone and cellulose nanowhiskers nanocomposite films for wound healing drug delivery application. J Biomed Mater Res A. 2017;105:2391–2404.
[46] Paiva MC, Ammar I, Campos AR, et al. Alfa fibers: mechanical, morphological and interfacial characterization. Compos Sci and Technol. 2007;67:1132–1138.
[47] Bai L, Gao Y, Li S, et al. Preparation and characterization of poly(vinylalcohol)/cellulose nanocomposites. Adv Mater Res. 2011;233–235:2383–2386.